

Supplementary Information

Wide diversity of methane and short-chain alkane metabolisms in uncultured archaea

Guillaume Borrel*, Panagiotis S. Adam, Luke J. McKay, Lin-xing Chen, Isabel Natalia Sierra-García, Christian M.K. Sieber, Quentin Letourneur, Amine Ghoulane, Gary L. Andersen, Wen-Jun Li, Steven J. Hallam, Gerard Muyzer, Valéria Maia de Oliveira, William P. Inskeep, Jillian F. Banfield, and Simonetta Gribaldo*

*Corresponding author. E-mail: guillaume.borrel@pasteur.fr & simonetta.gribaldo@pasteur.fr

The file contains:

Supplementary Discussion

- Energy conservation and methanogenesis cofactor biosynthesis in NM3 and NM4
- Energy conservation in Methanonatronarchaeia and Verstraetearchaeota
- Energy conservation in 'Ca. Methanophagales' (ANME-1)
- Possible oxidation of ethyl- to acetyl- through the m-WL pathway in GoM-Arc1
- Proposed names for species, genera, families and orders in the 'Candidatus Methanoliparia'
- Evolutionary and functional aspects of six conserved markers (m4 to m9)
- Distribution of markers associated with MCR/MCR-like-containing archaea in other archaea

Supplementary References

Supplementary Table list

Supplementary Table 2

Supplementary Table 4

Supplementary Table 5

Supplementary Figures 1 to 13

Supplementary Discussion

Energy conservation and methanogenesis cofactor biosynthesis in NM3 and NM4: The predicted methanogenesis and associated energy conservation complexes of NM3 are mostly similar to Methanofastidiosales¹ (Supplementary Fig. 1), their closest related methanogens in the archaeal phylogeny (Fig. 1). Members of these two lineages share i) the HdrABC/MvhADG electron bifurcating complex using H₂ for the reduction of a low potential ferredoxin and the regeneration of CoM-SH and CoB-SH², and ii) the Ehb complex which may generate a chemiosmotic gradient from the reduction of protons using the reduced ferredoxins produced by the HdrABC/MvhADG complex (Fig. 3). At the difference of Methanofastidiosa, NM3 might not be limited to reduce methyl-compound with H₂, but could possibly use formate as an alternative electron donor. Indeed, a gene coding for a formate dehydrogenase (FdhA) is found in cluster with genes coding for HdrA and MvhD. With HdrBC, they might form an HdrABC/MvhD/FdhA electron bifurcating complex, reducing a low potential ferredoxin and regenerating CoM-SH and CoB-SH by using formate as electron donor. This type of electron bifurcating complex using formate instead of H₂ have been previously suggested in *Methanococcus maripaludis*³.

The presence of homologues of the ferredoxin:quinone oxidoreductase (Fqo-like) complex and of the HdrD subunit in NM4 suggests that it might be able to generate a chemiosmotic gradient from the reduction of heterodisulfides (CoM-S-S-CoB) by reduced ferredoxins, similarly to what was proposed for Methanomassiliicoccales⁴ (Supplementary Fig. 1). However, the NM4 MAG lacks the heterodisulfide reduction catalytic subunit (HdrB) of the HdrABC/MvhADG complex. If the gene coding for this subunit is not in the missing part of the MAG, this would imply an alternative way to conserve energy than in Methanomassiliicoccales (Fig. 3, Supplementary Table 1). An alternative metabolism for NM4, namely methanotrophy, might also be possible (McKay et al., submitted).

Both NM3 and NM4 lack coenzyme M biosynthesis genes (Supplementary Table 1), suggesting that they are dependent on the production of this coenzyme by other members of the community for growth. Auxotrophy for coenzyme M is not uncommon among methanogens⁵⁻⁸. More surprising is the absence in NM3 of the genes involved in F₄₃₀ biosynthesis (Supplementary Table 1), otherwise present in most methanogens (Table 2). These four genes could however be present in the missing region of this MAG.

Energy conservation in Methanonatronarchaeia and Verstraetearchaeota: Consistently with the first reported Methanonatronarchaeia genomes⁹, Mnatro-ASL MAG is predicted to encode cytochrome *b* for electron transport in the membrane (Fig. 3, Supplementary Table 1). This type of energy conservation has a narrow distribution among methanogens, having been so far restricted to Methanosarcinales¹⁰. In contrast to the Methanosarcinales, the Methanonatronarchaeia encode a three-subunit membrane-bound formate dehydrogenase (Fdh-N-like complex¹¹) allowing them to use formate as an electron donor (Fig. 3). Because they rely on cytochrome *b* and do not possess the electron bifurcating complex formed by the heterodisulfide-reductase (HdrABC) and [Ni-Fe] hydrogenase (MvhADG), Methanonatronarchaeia probably do not reduce low potential ferredoxins during methanogenesis (Fig. 3). However, reduced ferredoxins are needed for anabolic reactions such as the synthesis of pyruvate from acetyl-CoA. Two Methanonatronarchaeia, including Mnatro-ASL, encode a hydrogen-evolving membrane-bound hydrogenase (Mbh) complex

(Fig. 3, Supplementary Table 1). This complex was initially characterized in Thermococcales where it couples the reduction of proton (H_2 evolution) by reduced ferredoxin with the generation of a sodium ion gradient^{12,13}. In Methanonatronarchaeia, the Mbh complex might function in the reverse direction, using H_2 and the chemiosmotic gradient to generate the reduced ferredoxin needed for anabolic reactions. This would correspond to a similar role played by Ech in *Methanosarcina barkeri* growing by reduction of methanol with H_2 ¹⁴.

Several subunits of the HdrABC/MvhADG complex appear to be absent in all known Verstraetearchaeota (corresponding to the '*Ca. Methanomethyliales*' order). Strikingly, the HdrA subunit responsible for electron bifurcation and reduction of ferredoxin^{2,15} is absent, as well as MvhD linking HdrA to MvhAG¹⁶. Distant homologues of the genes coding for the MvhAG hydrogenase are present but they likely correspond to the hydrogenase subunit (*hyhLS*) genes of a sulfhydrogenase complex (reducing H^+ or S^0 or S_n^{2-} with NADPH)^{17,18} as they are co-localized with the *hyhGB* genes. This HyhBGSL complex has been proposed to be involved in the disposal of excessive reducing equivalent produced during fermentation¹⁸, supporting previous metabolic predictions that Verstraetearchaeota have the potential to generate energy from fermentation in addition to methanogenesis¹⁹. Finally, the *hdrBC* genes (HdrB responsible for the reduction of CoM-S-S-CoB) are surrounded by genes coding for an uncharacterized membrane bound hydrogenase complex, suggesting an association between HdrBC and this complex (which we tentatively name Energy-converting Hydrogenase D, Ehd; Supplementary Fig. 2), rather than being part of a hypothetical HdrABC/MvhADG complex. We suggest that the Ehd complex couples the exergonic reduction of CoM-S-S-CoB by H_2 to the translocation of ions outside of the cell (Supplementary Fig. 2), which would resolve the energy conservation associated to methanogenesis in the absence of the HdrABC/MvhADG complex in the Verstraetearchaeota. However, as pointed out by Thauer et al.,²⁰ all membrane bound hydrogenase complexes known so far have a similar topology and couple the oxidation of H_2 with the translocation of ions within the cell (energy consuming reaction), which is the opposite of how Ehd would operate if it conserves energy by the reduction of CoM-S-S-CoB with H_2 .

Similarly to Methanonatronarchaeia, the absence of the HdrABC/MvhADG complex in Verstraetearchaeota MAGs (all members of '*Ca. Methanomethyliales*') likely prevents the reduction of low potential ferredoxins during methyl-dependent hydrogenotrophic methanogenesis. The ferredoxins needed for several anabolic reactions may be produced by the Energy-converting Hydrogenase B (Ehb) complex, which is encoded by all Verstraetearchaeota ('*Ca. Methanomethyliales*') MAGs (Fig. 3). Alternatively, if Verstraetearchaeota members are able to grow fermentatively, the ferredoxins reduced by the 2-oxoacid:ferredoxin oxidoreductases (Kor, Ior, Por and Vor) during amino-acid fermentation could be reoxidized by the Ehb complex, evolving H_2 and coupling the reaction to energy conservation by translocating sodium across the membrane. In addition, the Fpo-like complex, also encoded by all Verstraetearchaeota ('*Ca. Methanomethyliales*'), could associate with HdrD, as previously proposed in Methanomassiliicoccales⁴. In this case, the ferredoxin reduced during fermentation could be used by Fpo/HdrD complex to reduce CoM-S-S-CoB, linking fermentation and methanogenesis on methyl-compound. However, the capacity of the Verstraetearchaeota for fermentation will need further exploration. Indeed several enzymes possibly involved in fermentation (e.g. Kor, Ior, Por and Vor for peptide fermentation) in these archaea¹⁹, are also largely distributed in other methanogens that use them in reverse for amino-acid biosynthesis²¹.

Energy conservation in ‘*Ca. Methanophagales*’ (ANME-1): Annotation of the ANME-1-THS MAG strengthens previous observations made for ‘*Ca. Methanophagales*’^{22,23}, including the absence of the FwdFG subunits of the formyl-methanofuran dehydrogenase and of the methylene-H₄MPT reductase (Mer) in the m-WL pathway (Supplementary Fig. 3). As suggested for ANME-1b²⁴, the genes coding for MetFV have the potential to compensate for the absence of Mer (Supplementary Fig. 3). However, the possible oxidoreductase related to MetFV and the electron transporter associated with it (e.g. ferredoxin, NAD, F₄₂₀) remain unknown. Beyond these similarities, the energy conservation is likely different in ANME-1-THS compared to ANME-1b (Supplementary Fig. 3). Indeed, there are two potential PsrABC-like complexes in ANME-1-THS. The molybdenum/selenocysteine-containing dehydrogenase subunit of one of them is likely involved in sulfur compound reduction, while it is not excluded that the other one could be a formate dehydrogenase. In addition to the presence of potential Psr-like complexes and the absence of c-type multiheme cytochromes, ANME-1-THS also differs from ANME-1b by the presence of an Rnf complex that could participate to chemiosmotic coupling. The Rnf complex was initially described in bacteria, including acetogens²⁵, where it couples the reduction of NAD⁺ by ferredoxin to the translocation of sodium ions across the membrane, generating a chemiosmotic gradient for the ATP-synthase. So far, this complex has only been identified in Methanosarcinaceae among Archaea²⁶. The Rnf complex present in Methanosarcinaceae differs from the bacterial version by using methanophenazine/menaquinone instead of NAD⁺ as electron acceptor²⁷ (Supplementary Fig. 6A). Interestingly, the Rnf complex of ANME-1-THS probably functions more similarly to the bacterial version than the Methanosarcinales version (Supplementary Fig. 6A). Indeed, the residues that are conserved in both the bacterial NADH oxidoreductase RnfC and the NADH oxidoreductase NuoF are also conserved in the ANME-1-THS RnfC (Supplementary Fig. 6C). These residues are not conserved in the Methanosarcinales RnfC (Supplementary Fig. 6C). In addition, the cytochrome c subunit specific to most Methanosarcinales (with the exception of ANME-2c) is not present in ANME-1-THS (Supplementary Fig. 6B). The role of this complex in ANME-1-THS remains unclear but could be related to energy conservation. Interestingly, a similar Rnf complex was found in both NM1 MAGs (Supplementary Fig. 6).

Possible oxidation of ethyl- to acetyl- through the m-WL pathway in GoM-Arc1: After the activation of the alkane into alkyl- by the MCR-like complex, the enzymes involved into the reduction of the alkyl- into an acyl- remain unknown in ‘*Ca. Syntrophoarchaeum*’²⁸ and GoM-Arc1. This oxidation could occur in GoM-Arc1 via the m-WL pathway, as speculated for ‘*Ca. Syntrophoarchaeum*’²⁸. In this case, the alkyl- moiety would be transferred from CoM-SH to H₄MPT by the MTR complex, followed by its sequential oxidation into acyl-H₄MPT by Mer, Mtd and Mch (Fig. 3). Interestingly, the two GoM-Arc1 MAGs encode a divergent MTR complex possibly indicative of an adaptation to the transfer of ethyl- from CoM to H₄MPT. The utilization of this pathway is still purely hypothetical and alternatively, yet unknown enzymes could mediate this process. In any case, if GoM-Arc1 members use ethane (CH₃CH₃), the oxidation of the ethyl- group would lead to an acetyl- group making the beta-oxidation pathway not needed. Then, the acetyl- group would have to be transferred to CoA, to form acetyl-CoA, which would be further oxidized into two CO₂ through the reverse WL pathway (Fig. 3).

Proposed names for species, genera, families and orders in the ‘Candidatus Methanoliparia’:

The 16S rRNA genes of the NM1a and NM1b MAGs share 81% identity with the closest members of other archaeal classes, which is in the range of the recently recommended values for class-level classification²⁹. Moreover, the 16S rRNA genes of these two MAGs share 87% identity with each other, corresponding to family-level classification²⁹. We thus propose that the two NM1 MAGs belong to two distinct families, ‘*Candidatus Methanoliparaceae*’ and ‘*Candidatus Methanollivieraceae*’ and with the proposed class ‘*Candidatus Methanoliparia*’.

Description of the proposed genus ‘*Candidatus Methanoliparum thermophilum*’

‘*Candidatus Methanoliparum thermophilum*’ (Me.tha.no.li.pa’rum. N.L. neut. n. *methanum* methane ; N.L. pref. *methano-*, pertaining to methane; Gr. adj. *liparos* fat, greasy; N.L. neut. n. *Methanoliparum* methane-producing/consuming organism present in oil-rich environments; ther.mo’phi.lum. Gr. fem. *therme* heat; N.L. neut. adj. *philum* (from Gr. neut. adj. *philon*) loving; N.L. neut. adj. thermophilum heat-loving). This organism is not cultured, and is represented by the near-complete MAG NM1a (type material) obtained from an enrichment culture (50°C) using biodegraded oil as inoculum from Brazil (Table 1). It is proposed to be capable of methanogenesis (or methanotrophy) and short-chain alkane/long-chain fatty acid oxidation and is possibly motile.

Description of the proposed genus ‘*Candidatus Methanolliviera hydrocarbonica*’

‘*Candidatus Methanolliviera hydrocarbonica*’ (Me.than.ol.li.vie’ra. N.L. masc. n. *methanum* methane ; N.L. pref. *methano-*, pertaining to methane; N.L. gen. masc. n. *olliviera*, of Ollivier, named after Dr. Bernard Ollivier; N.L. masc. n. *Methanolliviera* a methane-producing/consuming organism named in honor of Dr. Bernard Ollivier for his work on methanogens and microorganisms from oil rich environments; hy.dro.car.bo’ni.ca N.L. fem. adj. *hydrocarbonica* pertaining to hydrocarbons, referring to its presence in hydrocarbon-rich environments). This organism is inferred to be capable of methanogenesis (or methanotrophy) and short-chain alkane/long-chain fatty acid oxidation, possibly motile, not cultured, represented by the nearly complete MAG NM1b (type material) obtained from Santa Barbara Channel oil seeps (Table 1).

Description of the proposed family ‘*Candidatus Methanoliparaceae*’

(Me.tha.no.li.pa.ra.ce’ae. N.L. neut. n. *Methanoliparum* a (Candidatus) genus name; *-aceae* ending to denote a family) N.L. neut. pl. n. *Methanoliparaceae* the (Candidatus) *Methanoliparum* family. The description is the same as for the candidate type genus *Methanoliparum*.

Description of the proposed family ‘*Candidatus Methanollivieraceae*’

(Me.than.ol.li.vie.ra.ce’ae. N.L. fem. n. *Methanolliviera* a (Candidatus) genus name; *-aceae* ending to denote a family; N.L. fem. pl. n. *Methanollivieraceae* the (Candidatus) *Methanolliviera* family) The description is the same as for the candidate type genus *Methanolliviera*.

Description of the proposed order ‘*Candidatus Methanoliparales*’

(Me.tha.no.li.pa.ra’les. N.L. neut. n. *Methanoliparum* a (Candidatus) genus name; *-ales* ending to denote an order) N.L. fem. pl. n. *Methanoliparales* the (Candidatus) *Methanoliparum*

order). The description is the same as for the candidate type genus *Methanoliparum*. This candidatus order also contains the candidate genus *Methanolliviera*.

Description of the proposed class 'Candidatus Methanoliparia'

(Me.tha.no.li.pa'ria. N.L. neut. n. *Methanoliparum* a (Candidatus) genus name; *-ia* ending to denote a class: N.L. neut. pl. n. *Methanoliparia*, the (Candidatus) Methanoliparales class. The description is the same as for the candidate type order *Methanoliparales*.

Evolutionary and functional aspects of six conserved markers (m4 to m9) in MCR/MCR-like bearing archaea: Six of the most conserved markers in all methanogens, methanotrophs and short-chain alkane oxidizers (m4-m9; Table 2) are encoded by genes that are co-localized in most reference genomes and MAGs (Supplementary Fig. 9). A congruence analysis among the single phylogenies of these markers revealed that they have a similar evolutionary history (Methods). '*Ca. Methanophagales*' (ANME-1) and GoM-Arc1 represent an exception, because m4, m8 and m9 show a different evolutionary history than m5, m6 and m7. These markers were thus concatenated separately for these MAGs. NM1a, NM1b and '*Ca. Syntrophoarchaeum caldarius*' have an extra-copy of the markers m4, m8 and m9 (named m4', m8' and m9' on Supplementary Fig. 10) that were also added to the phylogenetic analysis in a separate concatenation, after checking them for congruence.

Overall, the phylogeny of the six markers (Supplementary Fig. 10) is more similar to the MCR/MCR-like phylogeny (Fig. 2) than to the reference archaeal phylogeny (Fig. 1). In particular, the clustering of most methyl-dependent hydrogenotrophic methanogens lineages in both m4-m9 and MCR/MCR-like phylogenies (Fig. 2) is not congruent with the phylogenetic relationships between those lineages in the reference phylogeny (Fig. 1). This suggests that the possible transfer of MCR between some of these lineages (see main text) was also associated with a transfer of the markers m4 to m9.

Markers m4, m8 and m9 seem to have specific functional interactions with MCR/MCR-like complexes, as suggested by the occurrence of extra copies (m4', m8' and m9') in archaea with two distant MCR homologues: in the NM1 MAGs which code for both an MCR and an MCR-like complex, and in '*Ca. Syntrophoarchaeum caldarius*' which harbors distantly related MCR-like complexes (Fig. 2, Supplementary Fig. 10). A comparison between the MCR/MCR-like phylogeny (Fig. 2) and that of m4-m9 (Supplementary Fig. 10) provides some clues about the possible associations among these enzymes. The MCR-like complex and the second copies m4', m8' and m9' markers of NM1 show the same sister lineages in their respective phylogenies (Fig. 2, Supplementary Fig. 10) and this is also true for the MCR complex and the m4-m9 cluster of NM1 (Fig. 2, Supplementary Fig. 10). This suggests that in NM1, the m4', m8' and m9' proteins could be associated with the MCR-like complex, whereas the m4, m8 and m9 proteins could be associated with the canonical MCR complex. Similarly, the m4', m8' and m9' markers of '*Ca. Syntrophoarchaeum caldarius*' could interact with the MCR-like complex that branches with GoM-Arc1, while m4, m8 and m9 could be associated with the MCR-like complexes that branches with Bathyarchaeota and NM1 (Fig. 2, Supplementary Fig. 10). A functional link between m4, m8 and m9 proteins and the MCR/MCR-like complexes is further suggested by the fact that in the phylogenies of these three markers (Supplementary Fig. 10), GoM-Arc1 and '*Ca. Methanophagales*' have a position similar than in the MCR/MCR-like phylogeny (Fig. 2), while the position of their m5, m6 and m7 markers is congruent to the reference phylogeny (Fig. 1). This suggests that the transfer of MCR from a member of the

Acherontia to 'Ca. Methanophagales' could have occurred together with a transfer of the m4, m8 and m9 genes.

Homology of three of these markers with characterized enzymes provides potential clues about their role: marker m4 shares homology with cyclophilins, which are involved in protein folding³⁰, suggesting that it might be involved in MCR subunit folding and assembly. Marker m7 might have an activation role since it shares distant similarity with the ATP-dependent activator protein. Finally, marker m9 shares a weak similarity with McrC (m11) which is part of the activation complex of MCR³¹, and these two markers possibly emerged from an early gene duplication in archaea (not shown). Markers m5, m6 and m8 share no similarity with other enzymes and their function remains unknown.

Distribution of markers associated with MCR/MCR-like-containing archaea in other archaea:

Several marker genes associated with MCR/MCR-like-containing archaea are present in a few archaeal lineages that do not have MCR/MCR-like complexes (Supplementary Table 3). For example, markers m15, m16 and m17 occur in some representatives of Archaeoglobales, in NRA7 (a novel lineage related to Archaeoglobales³²), in Lokiarchaeota/Thorarchaeota³³ (Asgard superphylum³⁴), in Hydrothermarchaeota³², a lineage sister to Methanomassiliicoccales ("Methanomassiliicoccales-related"), and in Theionarchaea³⁵ (Supplementary Table 3). To the exception of Lokiarchaeota/Thorarchaeota, these lineages are closely related to clades containing MCR-bearing archaea (Fig. 1). Phylogenies of these three markers are mostly unresolved (Supplementary Figs. 11-13), but they do not indicate that they arose in these archaea without MCR/MCR-like complexes through recent horizontal gene transfer from known archaea with a methane or short-chain alkane metabolism. Also, in these phylogenies a Methanomassiliicoccales-related lineage (without methane-metabolism) and the Methanomassiliicoccales are clustered together, suggesting the presence of these enzymes at least in their last common ancestor (Supplementary Figs. 11-13). The clustering of two Acherontia lineages, Theionarchaea (without methane-metabolism) and Methanofastidiosa, is also observed in the phylogeny of marker m16 (Supplementary Fig. 11). Altogether, these analyses suggest that these three genes could be remnants of a previously complete methane-related metabolism, and were possibly repurposed for other functions following loss of methanogenesis. It also appears that these three markers might have been transferred from Archaeoglobales to NM4 (Supplementary Figs. 11-13).

Finally, none of the markers display a distribution pattern matching with the presence of the H₄MPT m-WL pathway in archaea (Supplementary Table 3), suggesting that they are not interacting directly with this pathway.

Supplementary References

1. Nobu, M. K., Narihiro, T., Kuroda, K., Mei, R. & Liu, W.-T. Chasing the elusive Euryarchaeota class WSA2: genomes reveal a uniquely fastidious methyl-reducing methanogen. *ISME J.* **10**, 2478 – 2487 (2016).
2. Kaster, A.-K., Moll, J., Parey, K. & Thauer, R. K. Coupling of ferredoxin and heterodisulfide reduction via electron bifurcation in hydrogenotrophic methanogenic archaea. *Proc. Natl. Acad. Sci. U. S. A.* **108**, 2981–2986 (2011).
3. Costa, K. C. *et al.* Protein complexing in a methanogen suggests electron bifurcation

- and electron delivery from formate to heterodisulfide reductase. *Proc. Natl. Acad. Sci.* **107**, 11050–11055 (2010).
4. Lang, K. *et al.* New mode of energy metabolism in the seventh order of methanogens as revealed by comparative genome analysis of ‘Candidatus Methanoplasma termitum’. *Appl. Environ. Microbiol.* **81**, 1338–1352 (2015).
 5. Bräuer, S. L., Cadillo-Quiroz, H., Yashiro, E., Yavitt, J. B. & Zinder, S. H. Isolation of a novel acidiphilic methanogen from an acidic peat bog. *Nature* (2006). doi:10.1038/nature04810
 6. Taylor, C. D., McBride, B. C., Wolfe, R. S. & Bryant, M. P. Coenzyme M, essential for growth of a rumen strain of *Methanobacterium ruminantium*. *J. Bacteriol.* (1974).
 7. Cadillo-Quiroz, H., Yavitt, J. B. & Zinder, S. H. *Methanosphaerula palustris* gen. nov., sp. nov., a hydrogenotrophic methanogen isolated from a minerotrophic fen peatland. *Int. J. Syst. Evol. Microbiol.* (2009). doi:10.1099/ijss.0.006890-0
 8. Sprenger, W. W., Van Belzen, M. C., Rosenberg, J., Hackstein, J. H. P. & Keltjens, J. T. *Methanomicrococcus blatticola* gen. nov., sp. nov., a methanol- and methylamine-reducing methanogen from the hindgut of the cockroach *Periplaneta americana*. *Int. J. Syst. Evol. Microbiol.* (2000). doi:10.1099/00207713-50-6-1989
 9. Sorokin, D. Y. *et al.* Discovery of extremely halophilic, methyl-reducing euryarchaea provides insights into the evolutionary origin of methanogenesis. *Nat. Microbiol.* **2**, 17081 (2017).
 10. Thauer, R. K., Kaster, A.-K., Seedorf, H., Buckel, W. & Hedderich, R. Methanogenic archaea: ecologically relevant differences in energy conservation. *Nat. Rev. Microbiol.* **6**, 579–591 (2008).
 11. Jormakka, M., Törnroth, S., Byrne, B. & Iwata, S. Molecular basis of proton motive force generation: Structure of formate dehydrogenase-N. *Science*. **295**, 1863–1868 (2002).
 12. Sapro, R., Bagramyan, K. & Adams, M. W. W. A simple energy-conserving system: proton reduction coupled to proton translocation. *Proc. Natl. Acad. Sci. U. S. A.* **100**, 7545–7550 (2003).
 13. McTernan, P. M. *et al.* Intact functional fourteen-subunit respiratory membrane-bound [NiFe]-hydrogenase complex of the hyperthermophilic archaeon *Pyrococcus furiosus*. *J. Biol. Chem.* **289**, 19364–19372 (2014).
 14. Meuer, J., Kuettner, H. C., Zhang, J. K., Hedderich, R. & Metcalf, W. W. Genetic analysis of the archaeon *Methanosarcina barkeri* Fusaro reveals a central role for Ech hydrogenase and ferredoxin in methanogenesis and carbon fixation. *Proc. Natl. Acad. Sci. U. S. A.* **99**, 5632–5637 (2002).
 15. Wagner, T., Koch, J., Ermler, U. & Shima, S. Methanogenic heterodisulfide reductase (HdrABC-MvhAGD) uses two noncubane [4Fe-4S] clusters for reduction. *Science*. **357**, 699–703 (2017).
 16. Stojanowic, A., Mander, G. J., Duin, E. C. & Hedderich, R. Physiological role of the F420-non-reducing hydrogenase (MvH) from *Methanothermobacter marburgensis*. *Arch. Microbiol.* **180**, 194–203 (2003).
 17. Kanai, T., Ito, S. & Imanaka, T. Characterization of a cytosolic NiFe-hydrogenase from the hyperthermophilic archaeon *Thermococcus kodakaraensis* KOD1. *J. Bacteriol.* **185**, 1705–1711 (2003).
 18. Ma, K., Schichot, R. N., Kellyt, R. M. & Adams, M. W. W. Hydrogenase of the hyperthermophile *Pyrococcus furiosus* is an elemental sulfur reductase or

- sulfhydrogenase: Evidence for a sulfur-reducing hydrogenase ancestor. *Biochemistry* **90**, 5341–5344 (1993).
19. Vanwonterghem, I. *et al.* Methylophilic methanogenesis discovered in the novel archaeal phylum Verstraetearchaeota. *Nat. Microbiol.* **1**, 16170 (2016).
 20. Thauer, R. K. *et al.* Hydrogenases from methanogenic archaea, nickel, a novel cofactor, and H₂ storage. *Annu. Rev. Biochem.* **79**, 507–536 (2010).
 21. Tersteegen, A., Linder, D., Thauer, R. K. & Hedderich, R. Structures and functions of four anabolic 2-oxoacid oxidoreductases in *Methanobacterium thermoautotrophicum*. *Eur J Biochem* **244**, 862–868 (1997).
 22. Hallam, S. J. *et al.* Reverse methanogenesis: Testing the hypothesis with environmental genomics. *Science*. **305**, 1457–1462 (2004).
 23. Meyerdierks, A. *et al.* Metagenome and mRNA expression analyses of anaerobic methanotrophic archaea of the ANME-1 group. *Environ. Microbiol.* **12**, 422–439 (2010).
 24. Timmers, P. H. A. *et al.* Reverse Methanogenesis and Respiration in Methanotrophic Archaea. *Archaea* **2017**, (2017).
 25. Biegel, E. & Muller, V. Bacterial Na⁺-translocating ferredoxin:NAD⁺ oxidoreductase. *Proc. Natl. Acad. Sci.* **107**, 18138–18142 (2010).
 26. Welte, C. & Deppenmeier, U. Bioenergetics and anaerobic respiratory chains of acetoclastic methanogens. *Biochimica et Biophysica Acta - Bioenergetics* **1837**, 1130–1147 (2014).
 27. Schlegel, K., Welte, C., Deppenmeier, U. & Müller, V. Electron transport during acetoclastic methanogenesis by *Methanosarcina acetivorans* involves a sodium-translocating Rnf complex. *FEBS J.* **279**, 4444–4452 (2012).
 28. Laso-Pérez, R. *et al.* Thermophilic archaea activate butane via alkyl-coenzyme M formation. *Nature* **539**, 396–401 (2016).
 29. Yarza, P. *et al.* Uniting the classification of cultured and uncultured bacteria and archaea using 16S rRNA gene sequences. *Nat. Rev. Microbiol.* **12**, 635–645 (2014).
 30. Wang, P. & Heitman, J. The cyclophilins. *Genome Biology* **6**, (2005).
 31. Prakash, D., Wu, Y., Suh, S. J. & Duin, E. C. Elucidating the process of activation of methyl-coenzyme M reductase. *J. Bacteriol.* **196**, 2491–2498 (2014).
 32. Jungbluth, S. P., Amend, J. P. & Rappé, M. S. Metagenome sequencing and 98 microbial genomes from Juan de Fuca Ridge flank subsurface fluids. *Sci. Data* **4**, (2017).
 33. Seitz, K. W., Lazar, C. S., Hinrichs, K.-U., Teske, A. P. & Baker, B. J. Genomic reconstruction of a novel, deeply branched sediment archaeal phylum with pathways for acetogenesis and sulfur reduction. *ISME J.* **10**, 1696–1705 (2016).
 34. Zaremba-Niedzwiedzka, K. *et al.* Asgard archaea illuminate the origin of eukaryotic cellular complexity. *Nature* **541**, 353–358 (2017).
 35. Lazar, C. S., Baker, B. J., Seitz, K. W. & Teske, A. P. Genomic reconstruction of multiple lineages of uncultured benthic archaea suggests distinct biogeochemical roles and ecological niches. *ISME J.* **11**, 1118–1129 (2017).

Supplementary tables

Supplementary Table 1: Presence/absence of genes involved in specific substrate utilization, energy metabolism, cofactor biosynthesis, secretion, sulfate assimilation, N₂ fixation, dissimilatory reduction of inorganic compounds, motility. Pathways and systems are subdivided into different spreadsheets. In each spreadsheet and for each MAG, protein accession numbers with the same color indicate co-localized genes. Provided in a separate .xls file.

Supplementary Table 2: arCOG annotation of the 38 markers previously defined as specific to Class I/II methanogens and the annotation as “methanogenesis markers” (1 to 17) by TIGRFAM.

Supplementary Table 3: Occurrence in archaea of 38 genes previously suggested to be methanogenesis marker. Provided in a separate .xls file.

Supplementary Table 4: Methods (sequencing/read assembly/contig binning) applied to obtain the ten MAGs presented in this study.

Supplementary Table 5: List of single copy genes composing the multi-marker concatenation used to build the Archaea reference tree (Fig. 1).

Supplementary Table 6: Genomes used to build the Archaea reference tree (Fig. 1). The first spreadsheet shows the number of genome available and selected for the phylogeny, and the second spreadsheet give the NCBI accession number (if any) of the selected genomes. Provided in a separate .xls file.

Supplementary Table 2: arCOG annotation of the 38 markers previously defined as specific to Class I/II methanogens and the annotation as “methanogenesis markers” (1 to 17) by TIGRFAM.

#	Marker Name	arCOG	TIGRFAM "methanogenesis markers"	Function
1	m1_mcrA	arCOG04857		MCR
2	m2_mcrB	arCOG04860		
3	m3_mcrG	arCOG04858		
4	m4_Predicted rotamase	arCOG04900	Methan_marker_3	Unknown
5	m5_DUF2102	arCOG04901	Methan_marker_6	Unknown
6	m6_DUF2112	arCOG04903	Methan_marker_5	Unknown
7	m7_YjiL-like	arCOG02679	Methan_marker_15	Unknown
8	m8_DUF2113	arCOG04904	Methan_marker_17	Unknown
9	m9_arCOG03226	arCOG03226	Methan_marker_7	Unknown
10	m10_atwA	arCOG00185		F430 bioS and activation
11	m11_mcrC	arCOG03225		
12	m12_mcrD	arCOG04859		
13	m13_cfbD	arCOG04888		
14	m14_cfbE	arCOG02822	Methan_marker_13	
15	m15_mtxX	arCOG00854	Methan_marker_4	Unknown
16	m16_AIR-synthase-related	arCOG00640	Methan_marker_2	Unknown
17	m17_Zn-ribbon protein	arCOG01116	Methan_marker_11	Unknown
18	m18_DUF2099	arCOG04893	Methan_marker_8	Unknown
19	m19_DUF2117	arCOG03231		Unknown
20	m20_Gly-thioamidase	arCOG02882	Methan_marker_1	PTM*
21	m21_DUF2124	arCOG04847		Unknown
22	m22_DUF2098	arCOG04846		Unknown
23	m23_SolubleP-type ATPase	arCOG01579		Unknown
24	m24_DUF2111	arCOG04902		Unknown
25	m25_arCOG04853	arCOG04853	Methan_marker_9	Unknown
26	m26_DUF2114	arCOG04866	Methan_marker_14	Unknown
27	m27_mtrA	arCOG03221		MTR
28	m28_mtrB	arCOG04867		
29	m29_mtrC	arCOG04868		
30	m30_mtrD	arCOG04869		
31	m31_mtrE	arCOG04870		
32	m32_arCOG04885	arCOG04885	Methan_marker_12	Unknown
33	m33_Arg-methyltransferase	arCOG00950	Methan_marker_10	PTM**
34	m34_DUF1894	arCOG04844		Unknown
35	m35_DUF1890	arCOG04845		Unknown
36	m36_DUF2115	arCOG03215		Unknown
37	m37_DUF2119	arCOG04894		Unknown
38	m38_DUF2121	arCOG03213		Unknown

MCR, methyl-coenzyme M reductase complex; MTR, N5-Methyltetrahydromethanopterin: coenzyme M methyltransferase complex;

PTM, involved in post-translational modification of McrA residues; F430 prosthetic group of MCR.

* Gly445, accroding to position on the MCR analysed by Ermler et al., 1997

** Arg271, accroding to position on the MCR analysed by Ermler et al., 1997

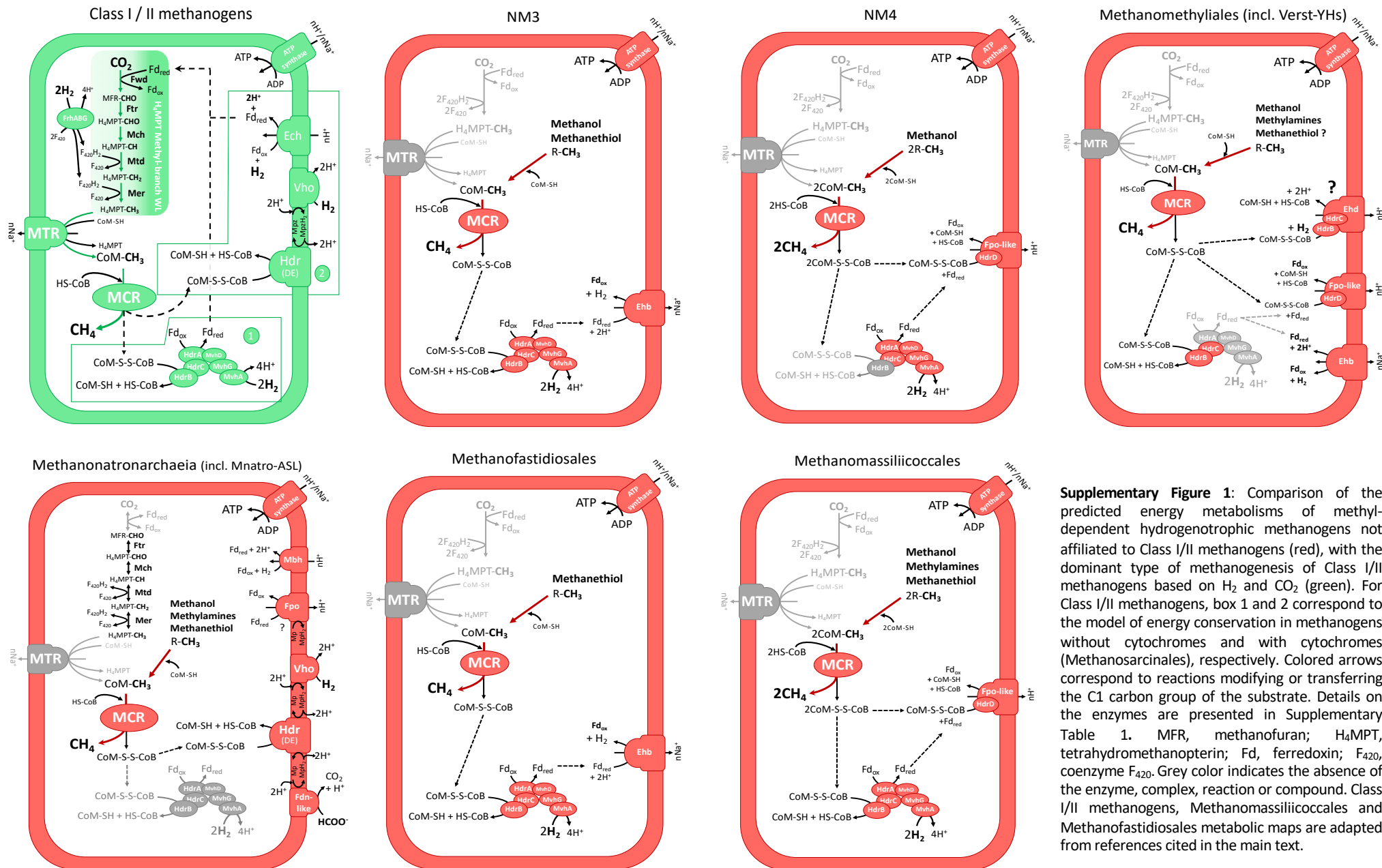
Supplementary Table 4: Methods (sequencing/read assembly/contig binning) applied to obtain the ten MAGs presented in this study.

MAG name	Sequencing technology	DNA fragment	Assembler (parameters)	Binning approach*
NM1a	HiSeq 2500	2 x 100 bp	MetaSPAdes (k=79)	ESOM (on 5-10 kb fragments of scaffolds > 5 kb)
NM1b		See Hawley et al., 2014		ESOM (on 3-5 kb fragments of scaffolds > 3 kb)
NM2	454 titanium	500 bp	Newbler (-mi 97 -ml 60)	MetaBAT (--sensitive)
NM3	HiSeq 2500	2 x 100 bp	Megahit (standart parameters)	MetaBAT2 (standart parameters)
NM4	HiSeq 2000	2 x 150bp	SOAPdenovo v1.05 (K=85,89,93,97,101,105)	ESOM (on 5-10 kb fragments of scaffolds > 5 kb)
Verst-YHS	HiSeq 2000	2 x 150bp	SOAPdenovo v1.05 (K=85,89,93,97,101,105)	ESOM (on 5-10 kb fragments of scaffolds > 5 kb)
Mnatro-ASL	HiSeq 2500	2 x 150bp	MetaSPAdes (standart parameters)	ESOM (on 5-10 kb fragments of scaffolds > 5 kb)
ANME-1-THS	HiSeq 2500	2 x 150 bp	IDBA-UD (--mink 20 --maxk 120 --step 10 --min_contig 300 --min_count 2 --pre_correction)	ESOM (on 3-5 kb fragments of scaffolds > 3 kb)
GoM-Arc1-GOS	HiSeq 2500	2 x 150 bp	IDBA-UD (--mink 20 --maxk 120 --step 10 --min_contig 300 --min_count 2 --pre_correction)	DAS_Tool with ABAWACA 1.07, MaxBin 2, CONCOCT, MetaBAT (all tools were run with standard parameter)
ANME-2c	HiSeq 2500	2 x 150 bp	IDBA-UD (--mink 20 --maxk 120 --step 10 --min_contig 300 --min_count 2 --pre_correction)	DAS_Tool with ABAWACA 1.07, MaxBin 2, CONCOCT, MetaBAT (all tools were run with standard parameter)

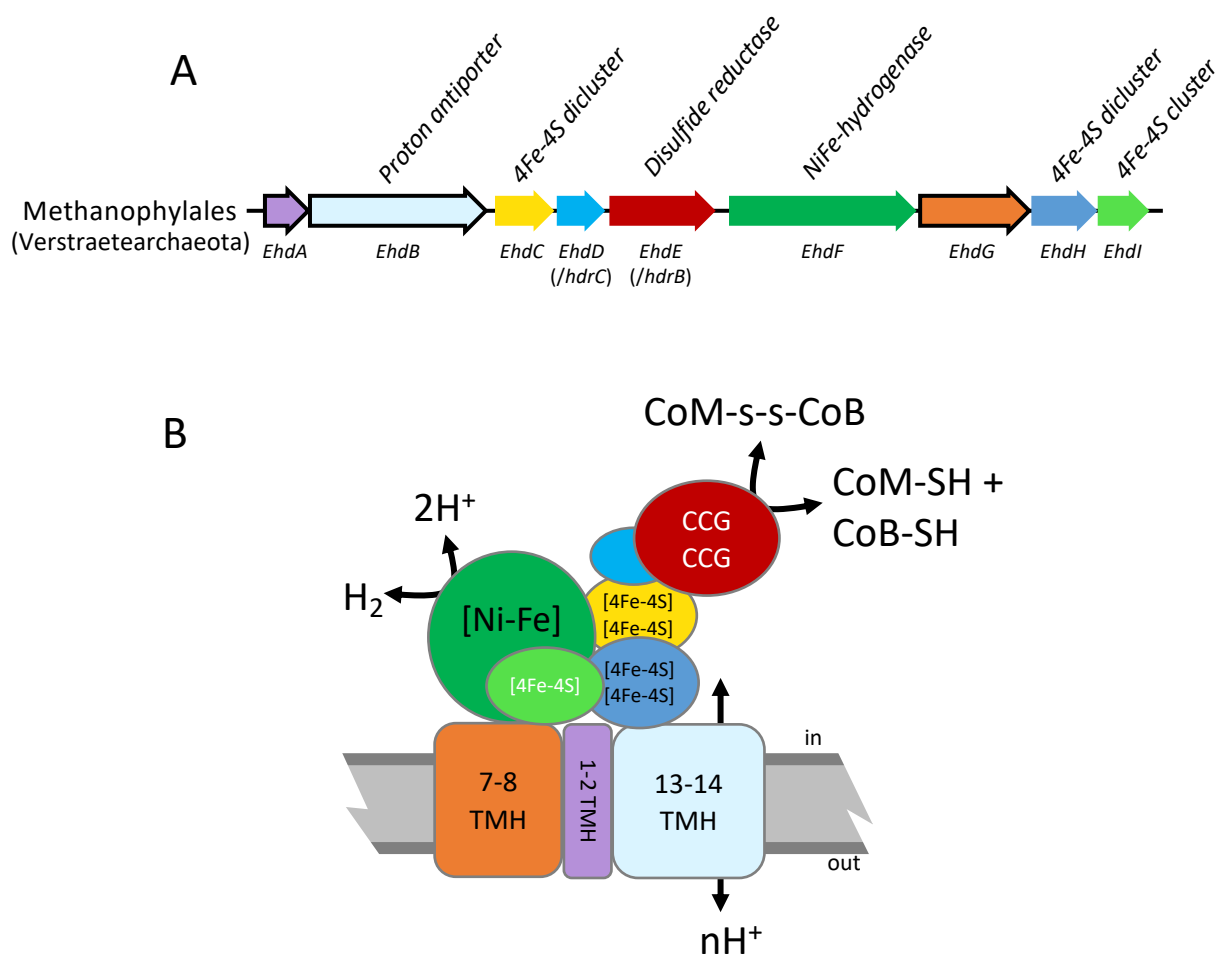
*For ESOM, tetranucleotide frequencies were transformed with the RobustZT method and the analysis was run with default values, with the exception of the training algorithm methods (k-batch), the number of columns and rows (changed according to esomWrapper.pl output), and the start value for radius (half the smaller length of the grid).

Supplementary Table 5: List of single copy genes composing the multi-marker concatenation used to build the Archaea reference tree (Fig. 1).

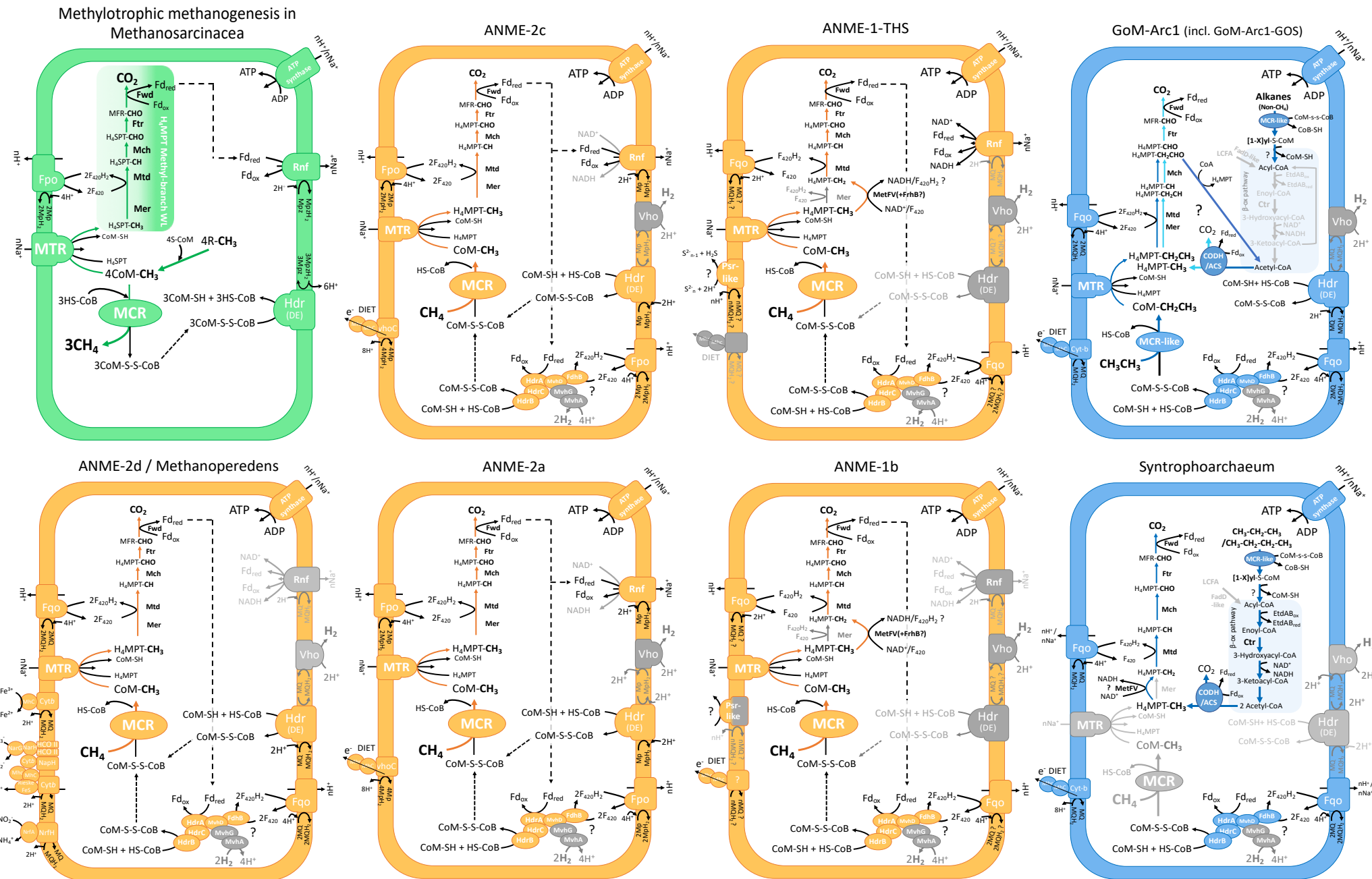
Name	COG
RNA polymerase A	COG0086
RNA polymerase B	COG0085
Ribosomal protein S2 rpsB	COG0052
Ribosomal protein S10 rpsJ	COG0051
Ribosomal protein L1 rplA	COG0081
Translation initiation factor IF 2	COG0532
Metalloendopeptidase	COG0533
Ribosomal protein L22	COG0091
Ribosomal protein L4/L1e rplD	COG0088
Ribosomal protein L2 rplB	COG0090
Ribosomal protein S9 rpsI	COG0103
Ribosomal protein L3 rplC	COG0087
Phenylalanyl tRNA synthetase beta subunit	COG0072
Phenylalanyl tRNA synthetase alpha subunit	COG0016
Ribosomal protein L14b/L23e rplN	COG0093
Ribosomal protein S5	COG0098
Ribosomal protein S19 rpsS	COG0185
Ribosomal protein S7	COG0049
Ribosomal protein L16/L10E rplP	COG0197
Ribosomal protein S13 rpsM	COG0099
Ribosomal protein L15	COG0200
Ribosomal protein L25/L23	COG0089
Ribosomal protein L6 rplF	COG0097
Ribosomal protein L11 rplK	COG0080
Ribosomal protein L5 rplE	COG0094
Ribosomal protein S12/S23	COG0048
Ribosomal protein L29	COG0255
Ribosomal protein S3 rpsC	COG0092
Ribosomal protein S11 rpsK	COG0100
Ribosomal protein L10	COG0244
Ribosomal protein S8	COG0096
tRNA pseudouridine synthase B	COG0130
Ribosomal protein L18P/L5E	COG0256
Ribosomal protein S15P/S13e	COG0184
Ribosomal protein S17	COG0186
Ribosomal protein L13 rplM	COG0102
Ribonuclease HII	COG0164
Ribosomal protein L24	COG0198
Ribosomal protein L30	COG1841
Ribosomal protein S4	COG0522



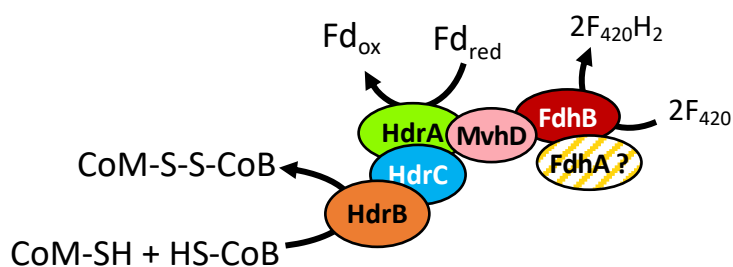
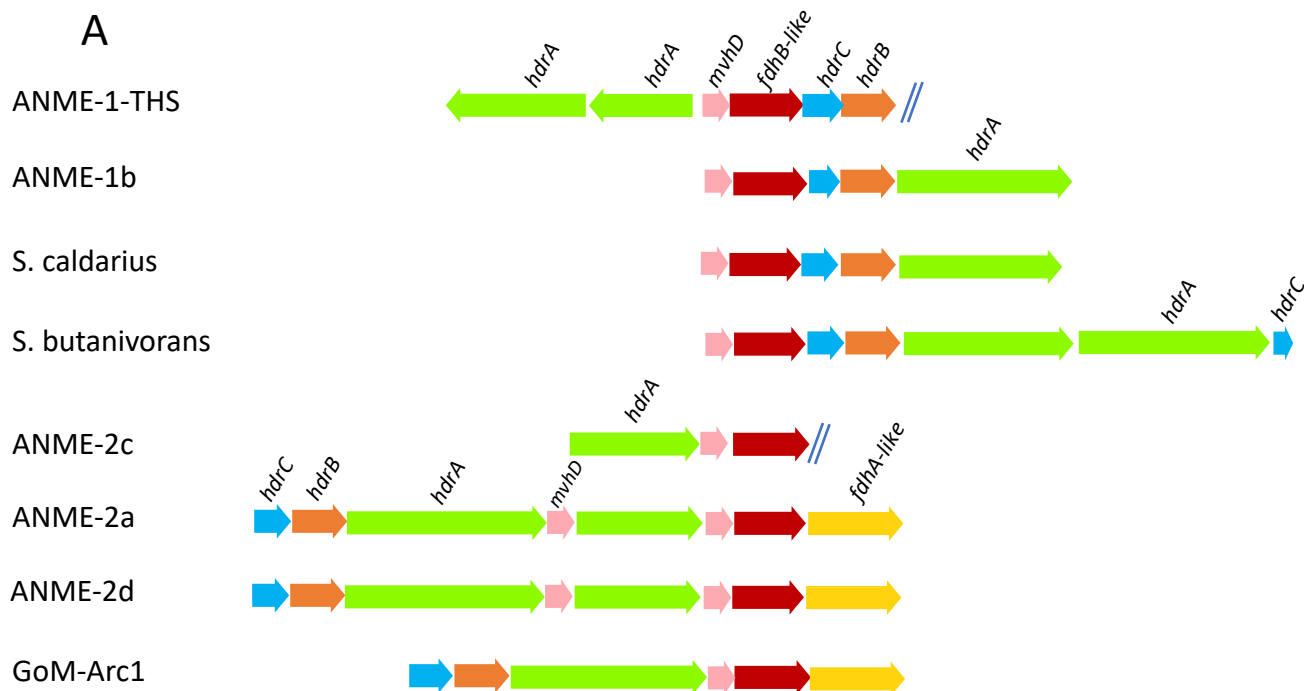
Supplementary Figure 1: Comparison of the predicted energy metabolisms of methyl-dependent hydrogenotrophic methanogens not affiliated to Class I/II methanogens (red), with the dominant type of methanogenesis of Class I/II methanogens based on H_2 and CO_2 (green). For Class I/II methanogens, box 1 and 2 correspond to the model of energy conservation in methanogens without cytochromes and with cytochromes (Methanosarcinales), respectively. Colored arrows correspond to reactions modifying or transferring the C1 carbon group of the substrate. Details on the enzymes are presented in Supplementary Table 1. MFR, methanofuran; H_4MPT , tetrahydromethanopterin; Fd, ferredoxin; F_{420} , coenzyme F_{420} . Grey color indicates the absence of the enzyme, complex, reaction or compound. Class I/II methanogens, Methanomassiliococcales and Methanofastidiosales metabolic maps are adapted from references cited in the main text.



Supplementary Figure 2: Energy-converting Hydrogenase D (Ehd). **A)** Gene organization of Ehd. Genes surrounded with a black frame have one or several predicted transmembrane helices, the number is indicated in the model below. **B)** Tentative model representing the possible redox coupling of Ehd. The annotation of the subunits is based on the detection of conserved motifs, with the exception of the proton antiporter subunit, which has been annotated according to overall similarity with a subunit of other complexes involved in proton translocation. EhdE possesses two cysteine rich regions (CCG) as in HdrB but slightly different from the given description of these motifs (C_{X32}CC_{X38}C in Verstraetearchaeota against C_{X31-39}CC_{X35-36}C). CoM-S-S-CoB, heterodisulfide; CoM-SH, coenzyme-M; CoB-SH, coenzyme B.

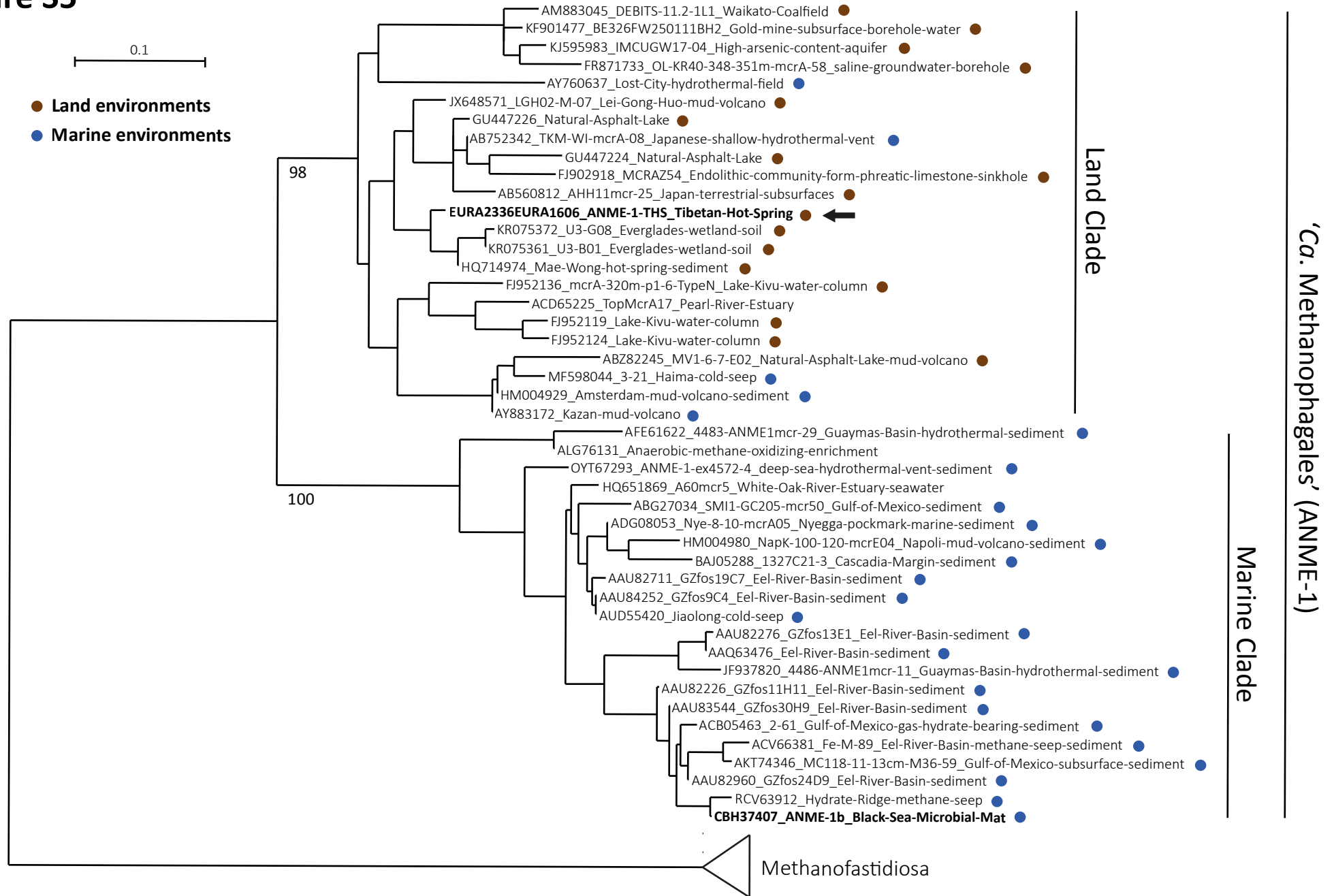


Supplementary Figure 3: Comparison of the predicted energy metabolisms of ANMEs (orange), short-chain alkane utilizers (blue) and methylophilic Methanosarcinaceae (green). Colored arrows correspond to reactions modifying or transferring the carbon group(s) of the substrate. Enzymes are detailed in Supplementary Table 1. MFR, methanofuran; H₄MPT, tetrahydromethanopterin; Fd, ferredoxin; F₄₂₀, coenzyme F₄₂₀; LCFA, Long chain fatty acids; MQ, menaquinone; Mp, methanophenazine; DIET, Direct Interspecies Electron Transfer. C-type multiheme cytochrome could possibly be involved in iron reduction associated with methanotrophy in Methanoperedens^{SUP36}. Grey color indicates the absence of the enzyme, complex, reaction or compound. ANME-2a/b/d, ANME-1b and 'Ca. Syntrophoarchaeum' metabolic maps are adapted from references cited in the main text.



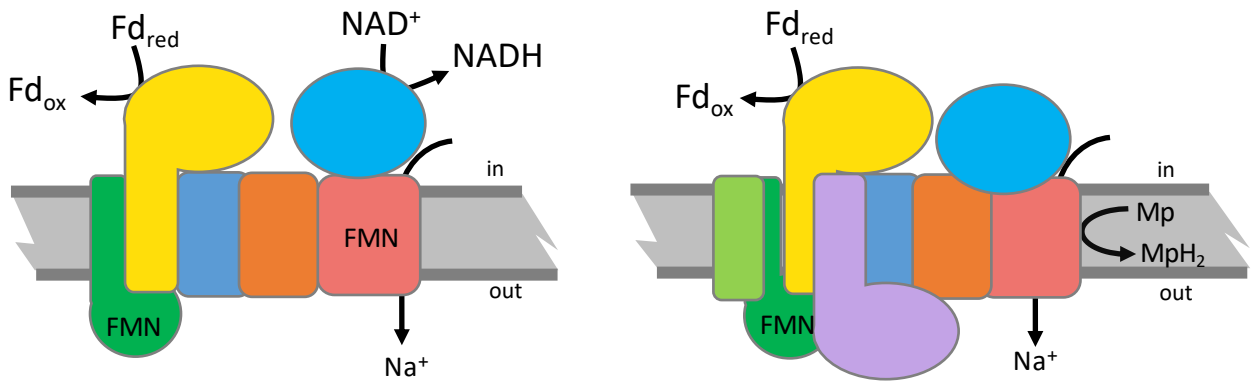
Supplementary Figure 4: The *hdrABC/mvhD/fdhB-like* gene cluster coding for a potential electron confurcating heterodisulfide reductase. **A)** Organization of the *hdrABC/mvhD/fdhB-like* gene clusters in ANME and short-chain alkane oxidizers. The F_{420} reducing hydrogenase domain of the FdhB-like enzyme is weakly conserved in ‘*Ca. Methanophagales*’ (ANME-1) and ‘*Ca. Syntrophoarchaeum*’ and highly conserved in ANME-2 and GoM-Arc1. In ANME-2 and GoM-Arc1, the *fdhB-like* gene is followed by a gene displaying similarity with *fdhA*. However, the formate dehydrogenase domain of this FdhA-like enzyme is weakly or not conserved. This *fdhA-like* gene is not present in ANME-2c but could be among the genes missing from the assembly as the contig is interrupted after the *fdhB-like* gene. Double dashes indicate contig interruption. **B)** Tentative model representing the possible redox coupling of HdrABC/MvhD/FdhB-like complex. Fd_{red} , reduced ferredoxin; Fd_{ox} , oxidized ferredoxin. CoM-S-S-CoB, heterodisulfide; CoM-SH, coenzyme-M; CoB-SH, coenzyme B.

Figure S5

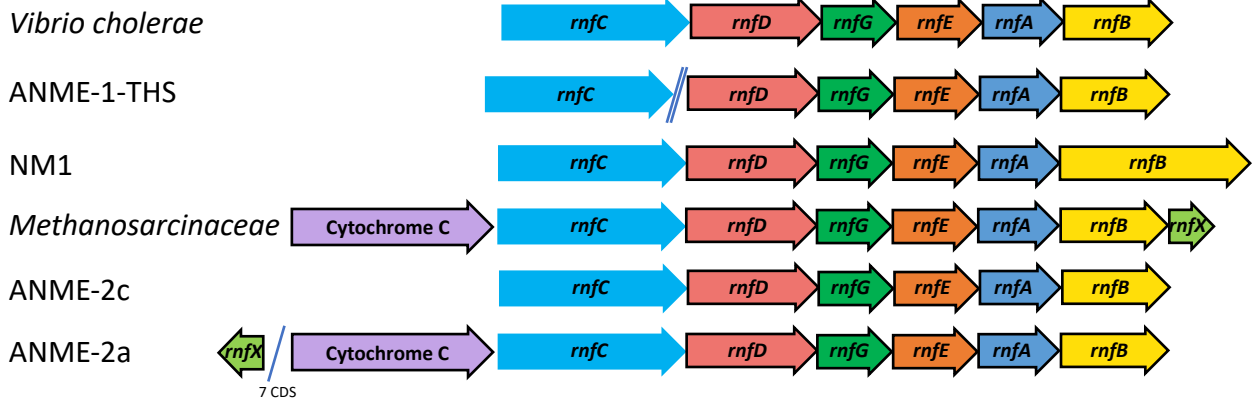


Supplementary Figure 5: Phylogeny and environmental distribution of 'Ca. Methanophagales' (ANME-1), highlighting a 'Ca. Methanophagales' Land Clade and a 'Ca. Methanophagales' Marine Clade. Sequences derived from marine environments are indicated by blue dots and those from terrestrial environments are indicated by brown dots. Sequences from the two 'Ca. Methanophagales' MAGs are in bold and an arrow indicates the ANME-1-THS MAG. The Maximum likelihood McrA tree was built with IQTREE^{Sup40} and the LG+G4 model on 53 sequences (45 sequences of ANME-1 and 8 sequences of *Methanofastidiosia* as outgroup). Node supports values were generated with 1000 ultrafast bootstrap replicates. Only the supports for the two main ANME-1 clades are displayed. The scale bar represents the average number of substitutions per site.

A



B



C

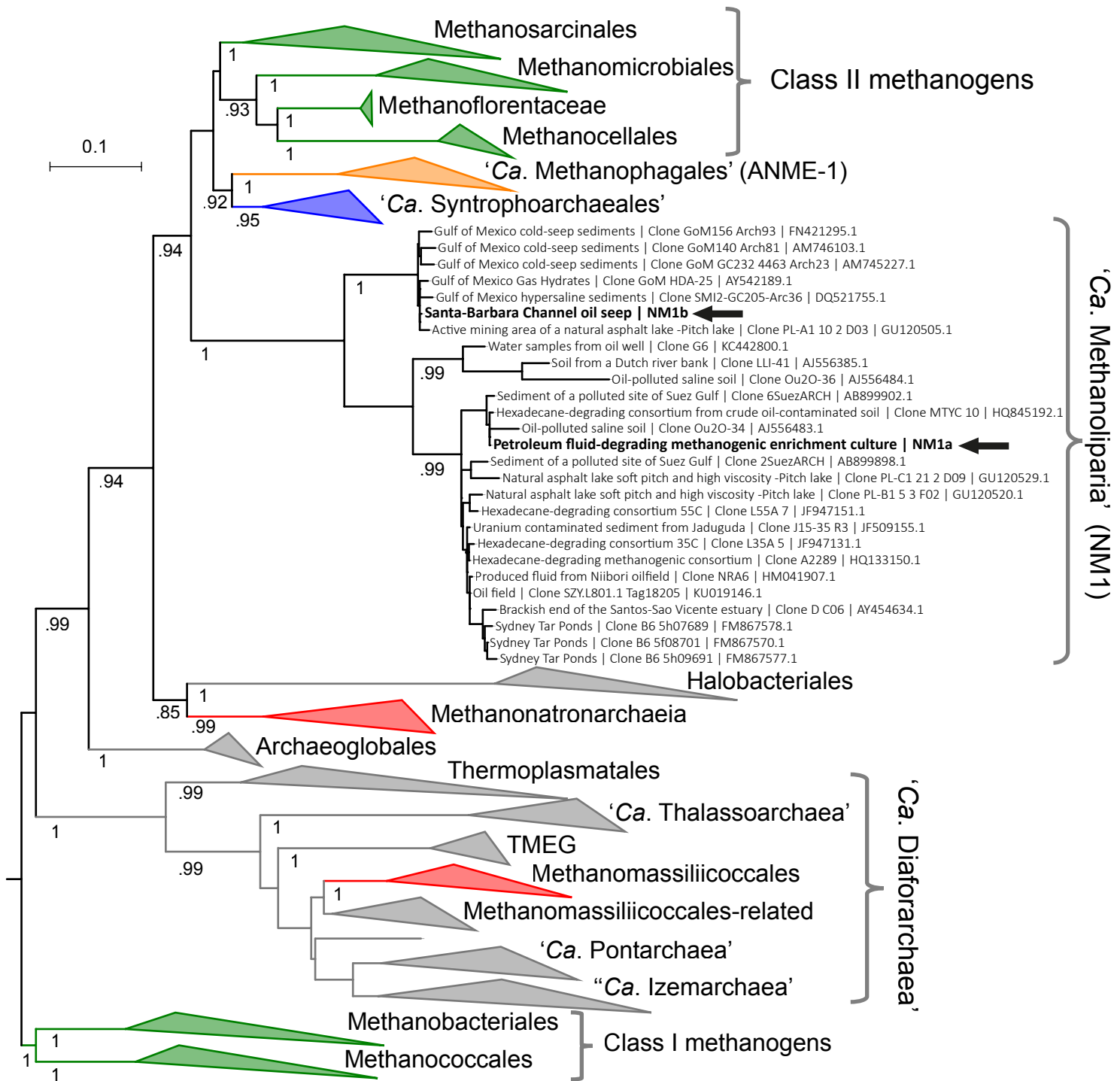
NuoF	<i>Escherichia coli</i>	G	L	K	G	R	G	G	A	G	F	S	T	G	L	K	W	S	L	M	P	K	D	E	S	M	N	I	R	Y	L	L	C	N	A	D	E	M	E	P	G	T	Y	K	D	R
RnfC	<i>Acetobacterium woodii</i>	G	I	V	G	L	G	G	A	T	F	P	T	H	V	K	L	A	I	-	-	P	P	D	-	K	K	V	D	C	V	V	L	N	G	A	E	C	E	P	Y	L	T	A	D	H
RnfC	<i>Vibrio cholerae</i>	G	I	S	G	M	G	G	A	G	F	P	T	A	K	K	L	-	-	Q	S	G	-	-	L	S	R	T	E	I	L	I	N	A	A	E	C	E	P	Y	I	T	A	D	D	
RnfC	<i>Rhodobacter capsulatus</i>	G	I	V	G	M	G	G	A	T	F	P	S	A	V	K	L	N	L	R	A	K	Y	-	-	-	D	L	T	T	L	I	I	N	G	A	E	C	E	P	Y	L	T	C	D	D
RnfC	ANME-1-THS	G	I	V	G	L	G	G	A	A	F	P	T	A	V	K	L	-	-	-	S	P	P	E	G	K	T	I	D	T	V	I	L	N	G	A	E	C	E	P	G	I	T	A	D	H
RnfC	NM1a	G	L	V	G	L	G	G	A	A	F	P	T	H	V	K	L	-	-	-	S	P	-	-	K	T	K	I	D	T	L	I	L	N	G	C	E	C	E	P	Y	I	T	S	D	H
RnfC	NM1b	G	V	V	G	L	G	G	A	A	F	P	T	S	V	K	L	-	-	-	S	P	-	-	D	K	I	D	T	L	I	I	N	G	C	E	C	E	P	Y	I	T	A	D	H	
RnfC	<i>Methanosarcina acetivorans</i>	G	I	V	E	Y	E	K	-	-	P	T	Y	L	A	L	-	-	-	K	P	-	-	G	K	R	I	D	T	L	L	M	N	A	T	F	-	-	P	L	I	T	H	A	Y	
RnfC	<i>Methanohalophilus halophilus</i>	G	I	V	E	N	Y	G	T	-	-	P	T	H	L	V	L	-	-	-	N	P	P	D	C	D	-	I	D	T	V	L	I	N	A	T	A	S	E	-	W	V	G	H	S	Y
RnfC	<i>Methanomethylovorans hollandica</i>	G	I	V	E	H	Y	G	L	-	-	P	T	Q	S	V	L	-	-	-	N	P	-	D	G	K	K	I	N	T	V	L	I	N	S	T	S	S	E	-	W	I	G	G	K	F
RnfC	ANME-2c	G	I	V	E	P	N	G	L	-	-	P	T	V	H	K	K	-	-	-	-	-	-	-	V	G	I	D	T	I	I	I	N	G	T	N	T	G	-	D	L	S	S	N	A	
RnfC	ANME-2a	G	V	V	E	L	N	G	Y	-	-	S	L	Y	N	M	L	T	S	E	-	-	-	-	K	L	I	D	T	V	L	I	N	L	S	F	S	G	-	D	V	S	S	N	C	

D

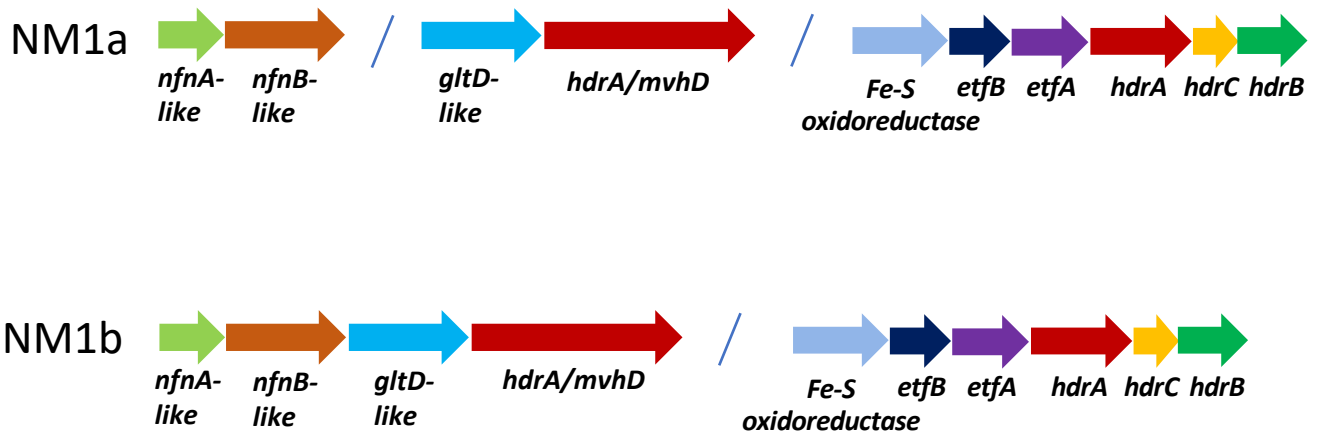
	<i>V. cholerae</i>	ANME-1-THS	NM1a	NM1b	<i>M.burtonii</i>	ANME-2c	ANME-2a
RnfA	6	6	6	6	6	6	6
RnfB	1	1	1	1	1	1	1
RnfC	0	0	0	0	0	0	0
RnfD	5	8	8	8	6	9	7
RnfE	5	6	6	6	6	6	6
RnfG	1	1	1	1	1	1	1
RnfX	-	-	-	-	3	-	2
Cyt-C	-	-	-	-	1	-	1

Supplementary Figure 6: The potential ferredoxin:NAD oxidoreductase Rnf complex coded by ANME-1-THS and NM1 genomes. **A)** On the left, tentative model of the ferredoxin:NAD⁺ oxidoreductase Rnf complex in Bacteria (based on^{Sup37}) and possibly in ANME-1-THS and NM1. On the right, tentative model of the ferredoxin:methanophenazine oxidoreductase Rnf complex in Methanosarcinales (based on^{Sup26}). The exact topology, electron flow and the sodium ion translocation mechanism has not been determined in Methanosarcinales. RnfG and RnfD of ANME-1-THS and NM1 have the FMN-binding domain characterized in *V. cholerae*^{Sup38}. In Methanosarcina FMN bind to RnfG^{Sup39} but RnfD does not have this domain^{Sup26}. The subunits are colored according to the genes in cluster organization (below). Fd_{red}, reduced ferredoxin; Fd_{ox}, oxidized ferredoxin; Mp, methanophenazine; MpH, reduced methanophenazine. **B)** Organization of the genes coding for Rnf. It includes distantly related species and shows the extra-subunit of the Methanosarcinales compared to the other taxa as well as the longer *rnfB* in NM1 (have 4 additional 4Fe-4S clusters). *rnfC* and *rnfD* of ANME-1-THS are on two contig edges. Genes surrounded with a black frame have one or several predicted transmembrane helices. **C)** Amino acid conservation in the NAD-binding domain in RnfC. Comparison between the NADH oxidoreductase (NuoF) of the NADH:quinone oxidoreductase complex (Nuo), the RnfC of bacteria known to bind NAD, the RnfC of Methanosarcinaceae known not to bind NAD and RnfC of ANME-1-THS and NM1. Conserved positions between NuoF and bacterial RnfC with a possible important function for binding NAD, are in green. They are mostly conserved in the RnfC of ANME-1-THS and NM1 suggesting that their Rnf complex use NAD, at the difference of the Rnf of the Methanosarcinaceae. **D)** Number of predicted transmembrane helices in Rnf subunits.

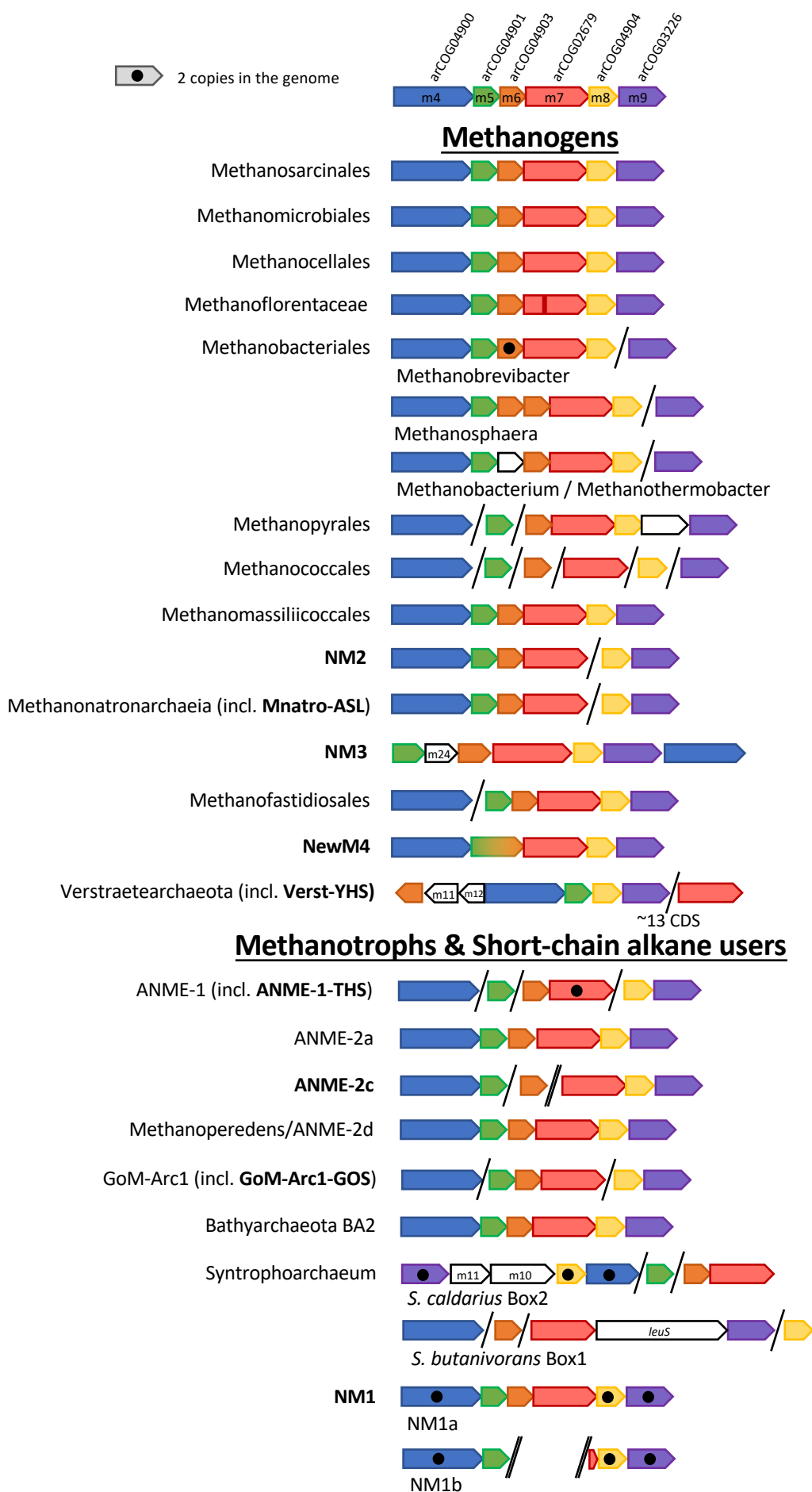
Figure S7



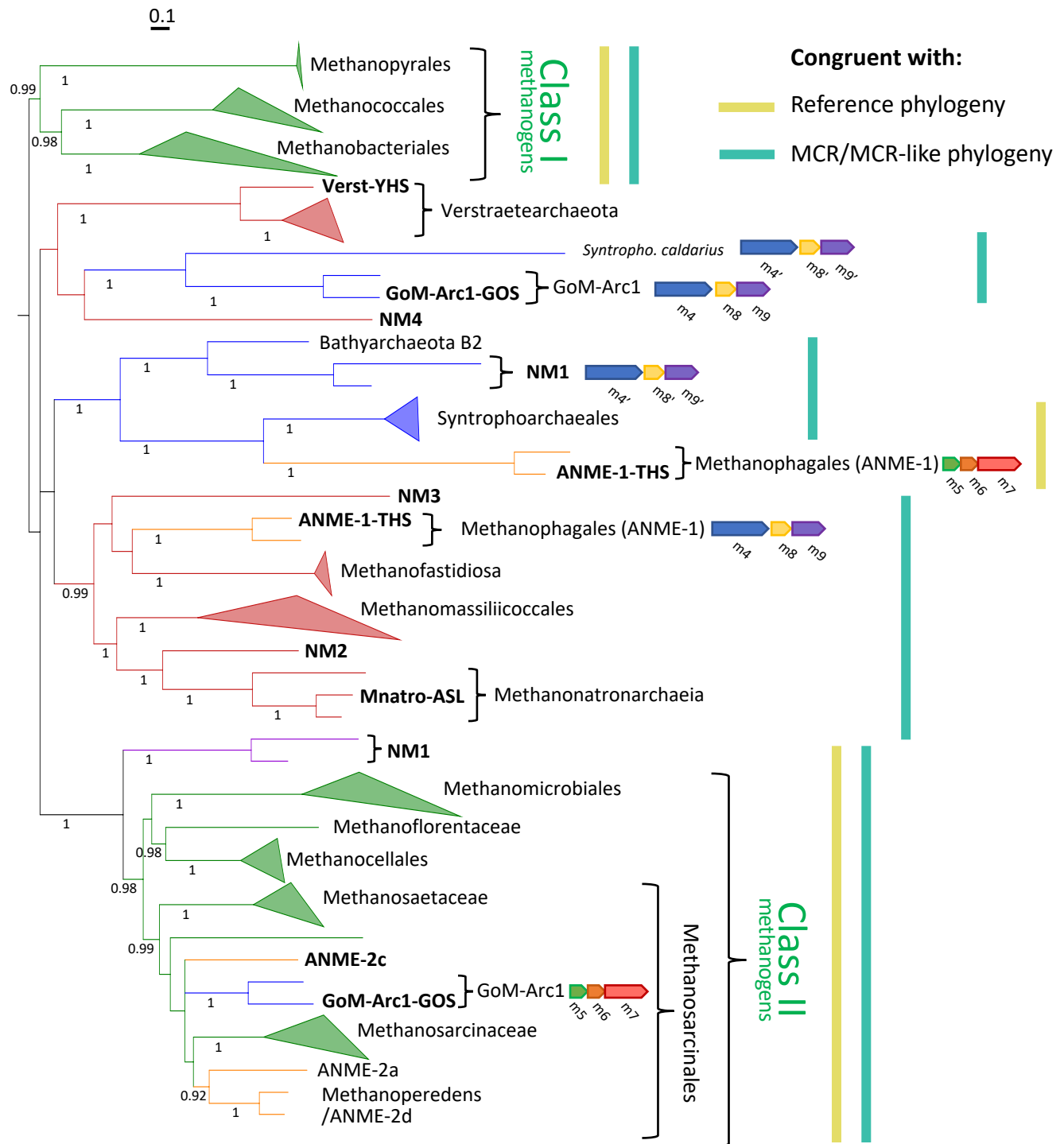
Supplementary Figure 7: Phylogeny, diversity and environmental distribution of NM1 ('Ca. Methanoliparia'). Black arrows indicate the position of the two NM1 MAGs. The Maximum likelihood 16S rRNA tree was built with IQTREE^{Sup40} and the GTR+G4 model on 197 sequences (27 sequences of 'Ca. Methanoliparia' and 170 sequences from other archaea). Node supports values were generated with 1000 ultrafast bootstrap replicates, and only values above 0.80 for main branches are shown. The scale bar represents the average number of substitutions per site.



Supplementary Figure 8: Gene clusters potentially encoding electron bifurcating/confurcating complexes in the two NM1 MAGs. These potential complexes correspond to NfnAB, HdrABC/EtfAB, HdrA/GltD-like enzyme (a fused *hdrBC* gene is present at another position in both NM1a and NM1b and might be associated to HdrA/GltD-like enzymes). Slashes indicate that some of the genes are not contiguous.




Supplementary Figure 9: Co-localization of the six markers (m4 to m9) with an unknown function but specifically present in MAGs/genomes encoding an MCR/MCR-like complex. Slashes indicate that some of the markers are not contiguous on the genome, double slashes indicate that this is possibly due to contig interruption, and dots indicate the makers that have a second occurrence in the MAG/genome.

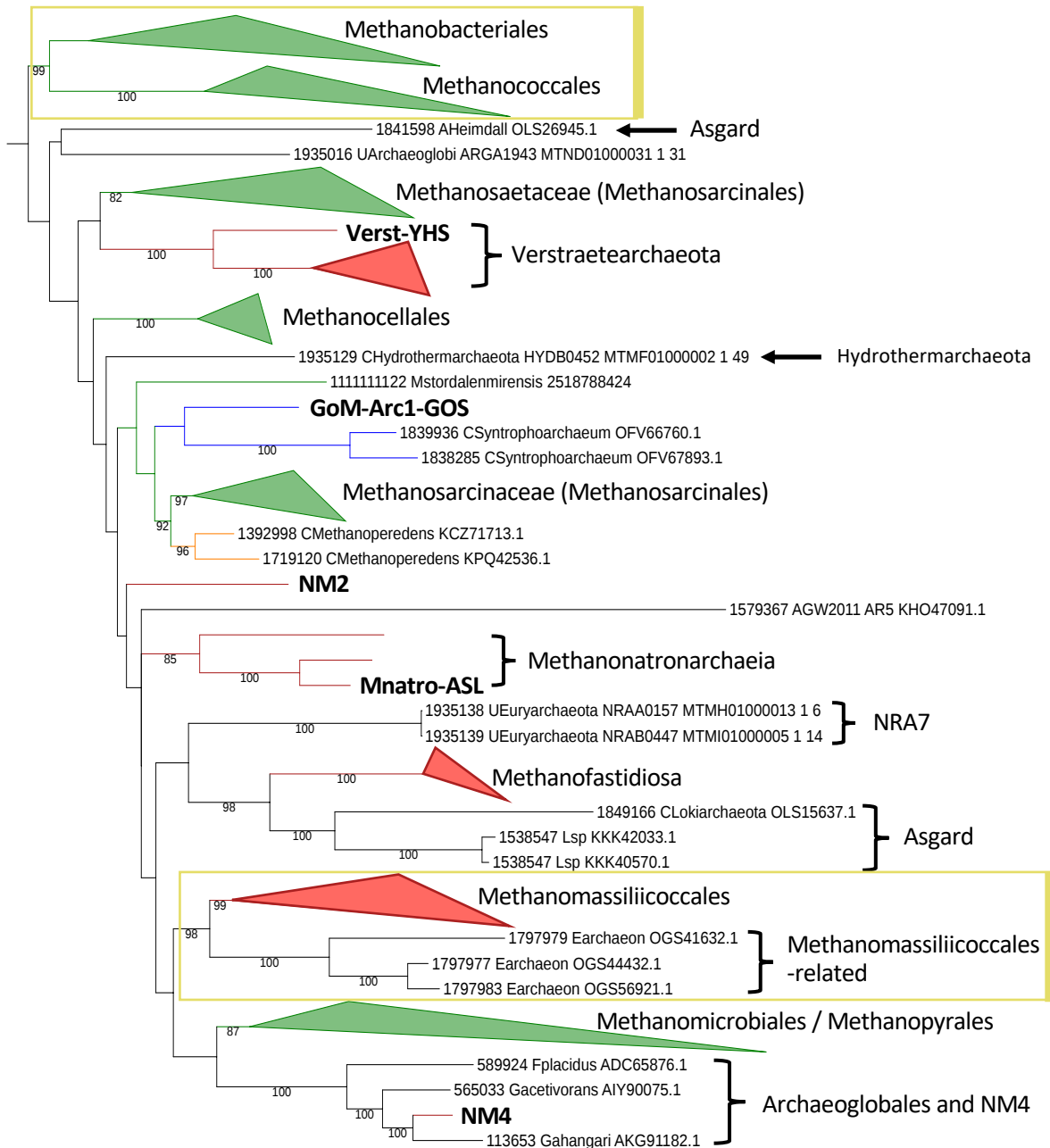


Supplementary Figure 10: Bayesian phylogeny (PhyloBayes, CAT+GTR+F4) based on a concatenation of markers m4 to m9 (1476 amino acid positions) from 109 MAGs/genomes. Node supports indicate posterior probabilities, and only values above 0.8 are shown. The scale bar represents the average number of substitutions per site. In the case of ANME-1 and GoM-Arc1 and for the extra copies of m4, m8, m9 that are present in NM1 and in '*Ca. Syntrophoarchaeum caldarius*' (*Syntropho. caldarius*), the markers concatenated are displayed in front of the corresponding branches. The color code of the lineages is similar to Fig. 1/Fig. 2. Vertical lines in front of the phylogeny indicate the portions of the tree that are congruent with the reference archaeal phylogeny (yellow) and/or the MCR/MCR-like subunits phylogeny (turquoise).

m15_mtxX (arCOG00854)

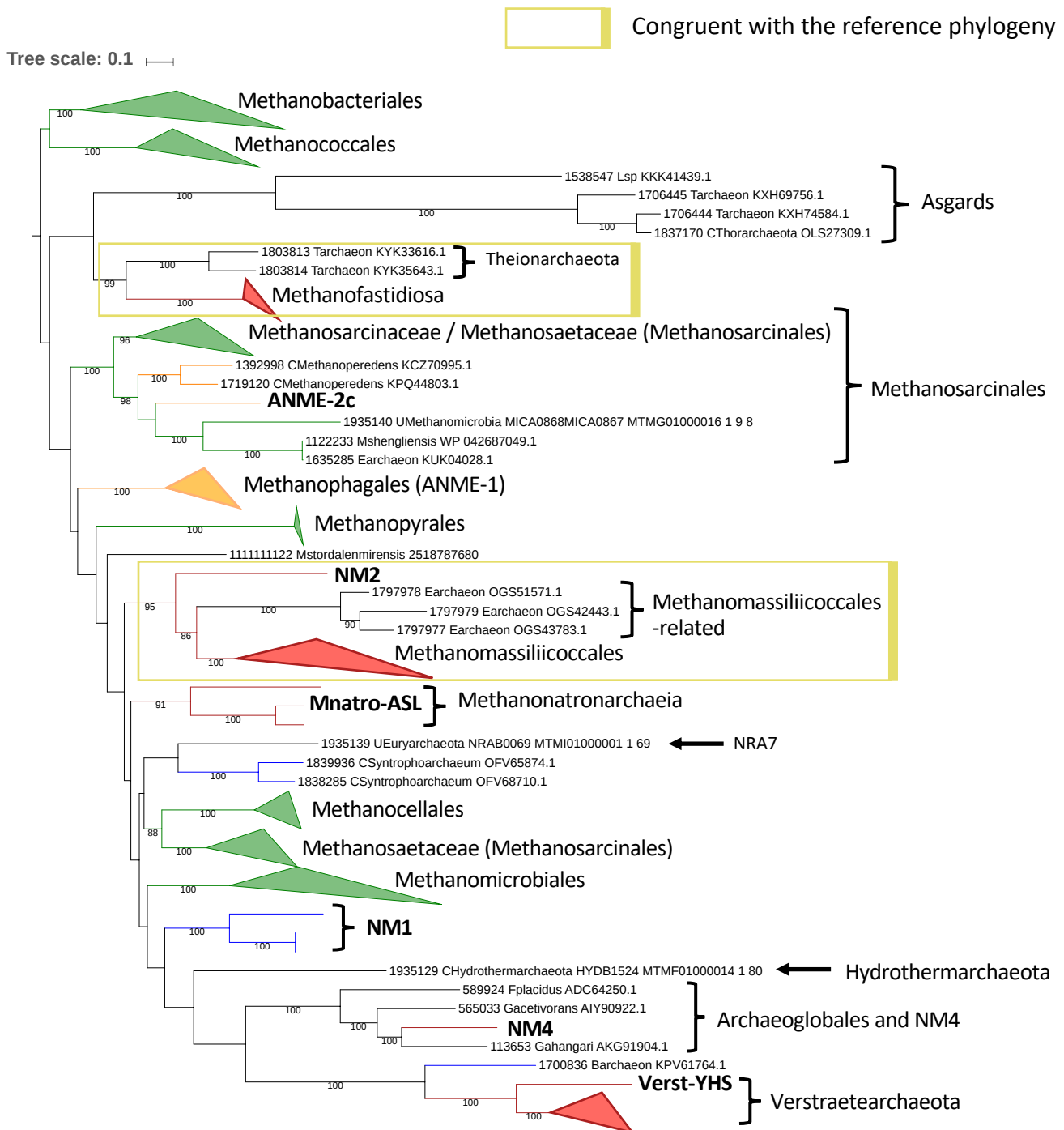
 Congruent with the reference phylogeny

Tree scale: 0.1



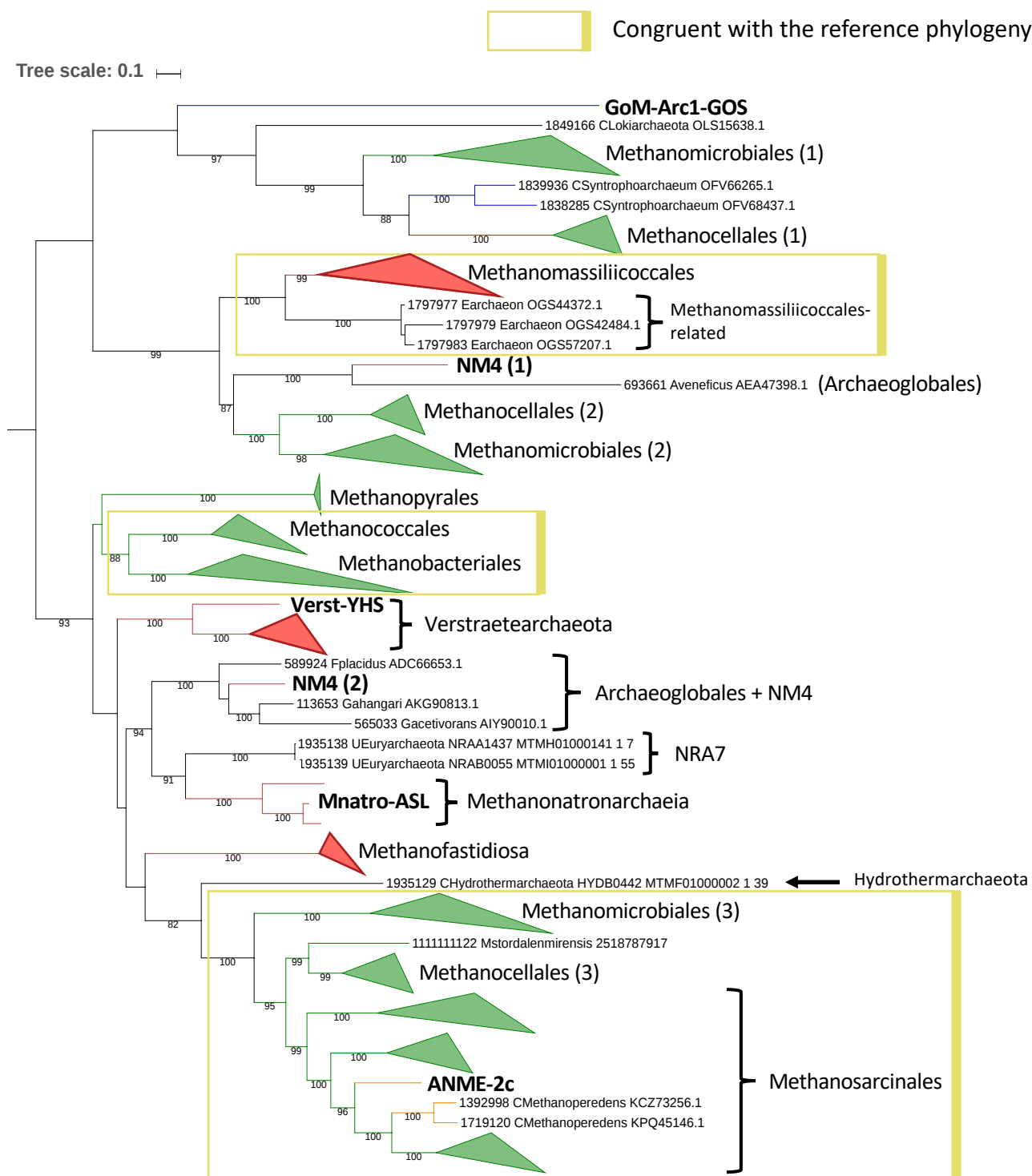
Supplementary Figure 11: Maximum likelihood phylogeny of the marker m15, mostly associated with archaea coding for MCR/MCR-like complexes but also present in few other archaea (based on 160 genomes/MAGs). The tree was built with IQTREE^{Sup40}, using the LG+R6 model (best model defined by IQTREE). Node supports were generated with 200 non-parametric bootstraps, and only values above 80% are shown. The yellow vertical lines in front of the phylogeny indicate the portions of the tree that are congruent with the reference archaeal phylogeny (Fig. 1). The scale bar represents the average number of substitutions per site.

m16_AIR synthase related (arCOG00640)



Supplementary Figure 12: Maximum likelihood phylogeny of the marker m16, mostly associated with archaea coding for MCR/MCR-like complexes but also present in few other archaea (based on 168 genomes/MAGs). The tree was built with IQTREE^{Sup40}, using the LG+R6 model (best model defined by IQTREE). Node supports were generated with 200 non-parametric bootstraps, and only values above 80% are shown. The yellow vertical lines in front of the phylogeny indicate the portions of the tree that are congruent with the reference archaeal phylogeny (Fig. 1). The scale bar represents the average number of substitutions per site.

m17_Zn-ribbon protein (arCOG01116)



Supplementary Figure 13: Maximum likelihood phylogeny of marker m17, mostly associated with archaea coding for MCR/MCR-like complexes but also present in a few other archaea (based on 155 genomes/MAGs). The tree was built with IQTREE^{Sup40}, using the LG+R6 model (best model defined by IQTREE). Node supports were generated with 200 non-parametric bootstraps, and only values above 80% are shown. The yellow vertical lines in front of the phylogeny indicate the portions of the tree that are congruent with the reference archaeal phylogeny (Fig. 1). The scale bar represents the average number of substitutions per site.